Apicomplexa-specific tRip facilitates import of exogenous tRNAs into malaria parasites

Tania Bour[a,1], Nassira Mahmoudi[a,1], Delphine Kapps[a,1], Sabine Thiberge[b], Daniel Bargieri[b,2], Robert Ménard[b], and Magali Frugier[a,3]

[a]Architecture and Reactivity of RNA, University of Strasbourg, CNRS, Institute for Molecular and Cellular Biology, 67084 Strasbourg Cedex, France; and [b]Malaria Biology and Genetics Unit, Pasteur Institute, 75015 Paris, France

The malaria-causing *Plasmodium* parasites are transmitted to vertebrates by mosquitoes. To support their growth and replication, these intracellular parasites, which belong to the phylum *Apicomplexa,* have developed mechanisms to exploit their hosts. These mechanisms include expropriation of small metabolites from infected host cells, such as purine nucleotides and amino acids. Heretofore, no evidence suggested that transfer RNAs (tRNAs) could also be exploited. We identified an unusual gene in *Apicomplexa* with a coding sequence for membrane-docking and structure-specific tRNA binding. This *Apicomplexa* protein—designated tRip (tRNA import protein)—is anchored to the parasite plasma membrane and directs import of exogenous tRNAs. In the absence of tRip, the fitness of the parasite stage that multiplies in the blood is significantly reduced, indicating that the parasite may need host tRNAs to sustain its own translation and/or as regulatory RNAs. *Plasmodium* is thus the first example, to our knowledge, of a cell importing exogenous tRNAs, suggesting a remarkable adaptation of this parasite to extend its reach into host cell biology.

tRNA | *Plasmodium* | trafficking

In *Plasmodium*, the causative agent of malaria, the nuclear genome has a minimal set of 45 transfer RNA (tRNA) genes, with only one gene per tRNA isoacceptor (1). This single-gene feature is an exception among eukaryotes, where tRNA genes are usually present in multiple copies. Discrepancies between codon use and expression levels of corresponding tRNAs were also observed in *Plasmodium falciparum* blood stages (2). These considerations raise the possibility that, under at least some conditions, the parasite may need an additional source of tRNAs and possibly rely on the import of exogenous tRNAs.

tRNA trafficking is only known to occur between compartments within eukaryotic cells. For example, nuclear-encoded tRNAs can transit from the nucleus to the cytoplasm, return to the nucleus, and be re-exported to the cytoplasm, depending on the tRNA maturation status and cellular environment (3). Cytoplasmic tRNAs are also imported into mitochondria (and chloroplasts) and participate in protein synthesis, mainly to supplement incomplete sets of organellar tRNAs (4). Which tRNAs are imported, and the mechanisms used for their transport, diverge considerably among organisms (5, 6). With these considerations in mind, we identified a *Plasmodium* genome-encoded protein that has motifs associated with tRNA binding. We show that this surface protein binds and imports exogenous tRNAs from the extracellular space into the parasite and that its deletion affects parasite development.

Results

Identification of *Plasmodium* tRip. A widely distributed tRNA binding motif is exemplified by a minimal tRNA binding protein—Trbp111—that was first identified in *Aquifex aeolicus* (7). This free-standing homodimeric protein specifically binds tRNA by recognizing its characteristic elbow structure. Other proteins that contain this motif include the yeast aminoacyl-tRNA synthetase cofactor 1 (ARC1p) (8), the metazoan AIMP1 (9), and *Toxoplasma gondii* Tg-p43 aminoacyl-tRNA synthetase interacting proteins (10).

Like Trbp111, ARC1p and AIMP1 bind tRNAs. Consistently, Tg-p43 is part of a multisynthetase complex, suggesting a tRNA-binding capability. We identified a gene encoding a 402-amino-acid *Plasmodium* protein (PF3D7_1442300 in *P. falciparum*) with a Trbp111-orthologous domain at its C terminus and an N-terminal region exhibiting a transmembrane helix motif (https://www.predictprotein.org:443/) (Fig. S1). Anticipating that this protein might import exogenous tRNAs, we designated it as tRip (tRNA import protein). We define tRip orthologs as proteins containing a C-terminal tRNA binding domain and a predicted transmembrane helix motif, which we found only in *Apicomplexa*, a phylum of parasitic protists that contains other human pathogens such as *Toxoplasma* and *Cryptosporidium*, in addition to *Plasmodium* (Fig. S2).

***P. falciparum* tRip Binds Human tRNAs.** In an in vitro assay, recombinant *P. falciparum* protein *Pf*tRip binds human native unfractionated tRNAs (Fig. 1*A*). The apparent dissociation constant (K_d) of 5 nM is of the same order of magnitude as that reported for Trbp111 (32 nM) (7) and ARC1p (5–10 nM) (11), and more than one order of magnitude lower than that observed for AIMP1 (200 nM) (12). To delineate *Pf*tRip tRNA binding activity, this experiment was repeated with fragments $Pf\text{tRip}_{1–174}$ (containing the transmembrane helix) and $Pf\text{tRip}_{214–402}$ (containing the Trbp111-like domain). Only the C-terminal module ($Pf\text{tRip}_{214–402}$) binds tRNAs, with an apparent K_d of 15 nM (Fig. 1 *B* and *C*). These experiments suggest that *Pf*tRip has a similar or higher affinity for tRNAs than Trbp111, ARC1p, and AIMP1 and that the C-terminal domain of the protein is responsible for this binding activity.

Significance

We identified a membrane protein that is unique to *Plasmodium* (malaria-causing parasite) and its phylogenetic family members. This protein is localized at the parasite's surface, binds transfer RNAs (tRNAs) specifically, and directs the import of exogenous tRNAs into the parasite. In the absence of this protein, the parasite's development is severely reduced. We propose that *Plasmodium* diverts tRNAs from host cells to support its life cycle and discuss the biological pertinence of this unprecedented host–pathogen interaction, as well as the possible fate of imported tRNAs.
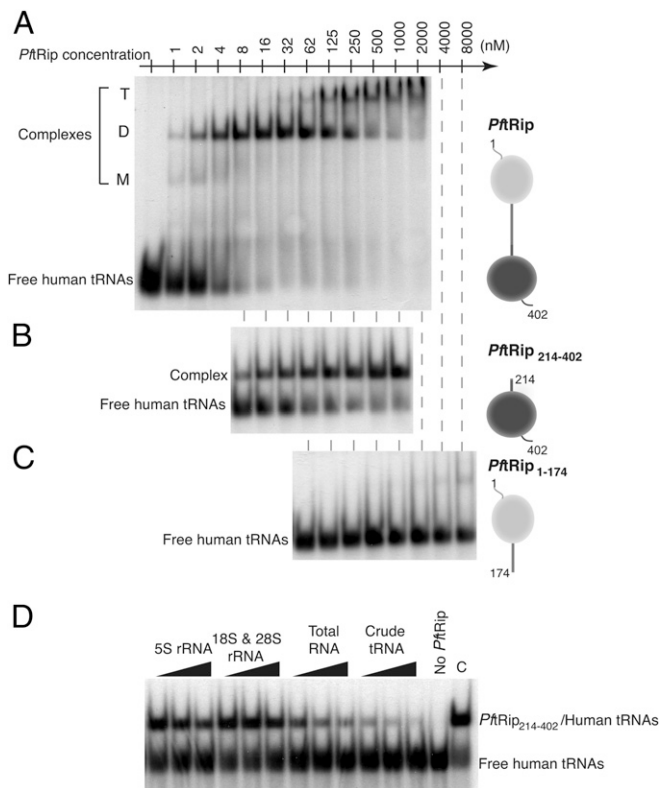
BIOCHEMISTRY

www.manaraa.com

Fig. 1. Binding capacity and specificity of recombinant *Pf*tRip for tRNAs. Band shift assays were performed with radiolabeled crude extracts of human tRNA and increasing concentrations of (*A*) *Pf*tRip, (*B*) *Pf*tRip$_{214–402}$, and (*C*) *Pf*tRip$_{1–174}$. Bound tRNAs were visible at three different positions corresponding to monomeric (M), dimeric (D), and tetrameric (T) forms of *Pf*tRip. (*D*) Competition assays were conducted in the presence of RNA from different species (*Xenopus laevis* 5S rRNA, calf liver 18S and 28S rRNAs, total human RNA and crude extracts of human tRNA). C, control experiment without RNA competitor.

To investigate the specificity of *Pf*tRip$_{214–402}$ for tRNAs compared with other RNAs, we conducted competition experiments with different pools of RNAs: (*i*) 5S ribosomal RNA (rRNA), (*ii*) 18S and 28S rRNAs, (*iii*) total RNAs, including tRNAs, and (*iv*) unfractionated tRNAs. Only extracts containing tRNAs (total RNAs or crude tRNAs) competed efficiently with a preformed complex between labeled human tRNAs and *Pf*tRip$_{214–402}$ (Fig. 1*D*). We then carried out an RNA footprinting analysis to identify contact points between *Pf*tRip and tRNAs. *Pf*tRip binds to the outside corner of the L-shaped tRNA molecule (Fig. S3 *A* and *B*). To further characterize tRNA recognition, we determined whether *Pf*tRip could still engage the tRNA in the yeast aspartyl-tRNA synthetase (AspRS)/tRNA^{Asp} complex (13). AspRS recognizes the "inside" of the L-shaped tRNA. This experiment showed that both *Pf*tRip and AspRS bind simultaneously to tRNA^{Asp} (Fig. S3*C*). The formation of this ternary complex confirms that *Pf*tRip binds only to the outside of the L-shaped tRNA structure. A similar ternary complex has been observed for tRNA^{Ile}, Trbp111, and isoleucyl-tRNA synthetase (14).

Expression and Subcellular Localization of tRip in *P. berghei*. The *Plasmodium* life cycle is complex, involving several parasite stages. The parasite multiplies in the midgut of the mosquito vector and inside hepatocytes (15) and erythrocytes (16) in the mammalian host (Fig. S4*A*). Analysis of transcriptomic and proteomic data from *P. falciparum* and *P. yoelii* (plasmodb.org/plasmo/) indicates that tRip is produced virtually constitutively during the parasite life cycle, i.e., in asexual and sexual blood stages (17–19), mosquito

forms (20), and pre-erythrocytic stages (21, 22). Likewise, *Toxoplasma* (23) or *Cryptosporidium* (24) transcriptomic databases do not show any significant variations in tRip mRNA expression. Immunofluorescence assays with purified anti-*Pf*tRip$_{214–402}$ antibodies (Fig. S4*B*) confirmed the presence of tRip in *P. berghei* extracellular ookinete and sporozoite stages and intracellular hepatocytic and erythrocytic stages (Fig. S4*C*).

Assays using salivary gland sporozoites revealed similar peripheral fluorescence staining for tRip and the major surface protein, CSP (circumsporozoite protein; Fig. 2*A*). As the sporozoite pellicle contains an outer membrane (plasma membrane) and two inner membranes, we used the differential solubility characteristics of these membranes toward Triton X-100 to more precisely localize tRip (25). In untreated sporozoites, the fluorescence signals generated by tRip and CSP were evenly distributed at the parasite periphery (Fig. 2*B*). Fluorescence at the periphery was lost following outer membrane disruption with Triton X-100. This observation demonstrates that tRip is anchored to the plasma membrane
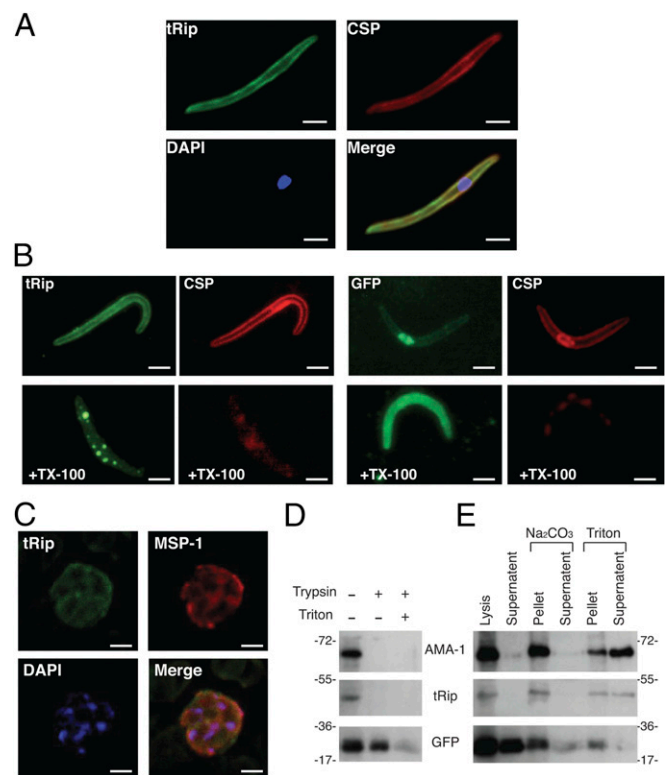

Fig. 2. tRip localization. (*A*) Coimmunolocalization assays on *P. berghei* sporozoites. The major sporozoite surface protein CSP and tRip were probed with anti-CSP antibodies and anti-*Pf*tRip$_{214–402}$, respectively, and the sporozoite nucleus was stained with DAPI. (*B*) Extraction of tRip with Triton X-100 (TX-100). TX-100 selectively removes the plasma membrane and its associated proteins (CSP and tRip), whereas the inner membrane complex is resistant to this treatment (25). Sporozoite integrity is shown by GFP staining, with CSP staining shown to verify successful Triton X-100 extraction. (Scale bars, 2 μm.) (*C*) Subcellular localization of tRip in asexual blood-stage parasites of *P. berghei*. The schizont of *P. berghei* was doubly labeled with mouse anti-MSP-1 antibody (surface marker, red) and rabbit anti-tRip antibody (green). Nuclei were visualized with DAPI (blue). (Scale bars, 5 μm.) (*D*) Protease protection assays on blood-stage parasites. Assays were performed with schizonts freed from erythrocytes, treated with trypsin, and probed with anti-*Pf*tRip$_{214–402}$ antibody. GFP was used as a cytosolic control, digested by trypsin only under denaturing conditions (+ Triton). (*E*) Carbonate vs. Triton extraction of membrane proteins from blood-stage parasites (schizonts). Both tRip and the apical membrane antigen 1 (AMA-1) (41) were found in the membrane pellet after Na$_2$Co$_3$ treatment and were released into the supernatant only on Triton treatment.

www.manaraa.com

of the sporozoite, presumably via its protein transmembrane helix motif (Fig. S1), thus enabling interaction with exogenous tRNAs.

Additionally, in blood-stage parasites, tRip and the surface protein MSP-1 colocalize (Fig. 2C). Protease protection assays on the parasite blood stage confirmed this cell surface localization (Fig. 2D) because signals corresponding to AMA-1 (apical membrane antigen 1) and tRip both vanished on trypsin treatment. Comparison of carbonate vs. detergent extraction showed that tRip behaves like AMA-1 and is only found in the reaction supernatant after Triton extraction and not after lysis or Na_2CO_3 treatment, indicating that it is an integral membrane protein (Fig. 2E).

Plasmodium Sporozoites Import Exogenous tRNAs. All *Apicomplexa* have in common the sporozoite stage. Unlike blood stages, the sporozoite is an accessible extracellular stage, which is characterized by its motility and its ability to traverse cells (26–28) without forming a parasitophorous vacuole. Thus, this parasite stage has an opportunity to directly interact with host tRNAs. For these reasons, we tested the ability of tRip to uptake exogenous tRNAs into *P. berghei* sporozoites. A FISH experiment was performed with *Escherichia coli* tRNA^{Val} and live or heat-treated sporozoites (50 °C for 30 min). Import of *E. coli* tRNA^{Val} was observed only in live WT parasites (Fig. 3A). tRNA import was also observed with sporozoites of two other *Plasmodium* species: *P. falciparum* and *P. yoelii* (Fig. 3A).

To examine whether this import is specific for tRNAs (as implied by the RNA binding assays above; Fig. 1D), live *P. berghei* sporozoites were incubated with Alexa Fluor-labeled in vitro-transcribed *E. coli* tRNA^{Val} and with human 5S rRNA (control). The fluorescent *E. coli* tRNA^{Val} transcript entered and accumulated inside the parasite, whereas the fluorescent 5S rRNA did not (Fig. S5). Radiolabeled full-length tRNAs from mouse hepatocytes (Hepa1-6 cells) were protected from extracellular RNase treatment inside live but not heat-treated sporozoites (Fig. 3B). Based on these results, we conclude that full-length tRNAs enter sporozoites by an active process.

In a first attempt to show that import was dependent on tRip, sporozoites were incubated with an anti-*Pf*tRip$_{214–402}$ antibody to block tRNA binding in a FISH experiment. The number of parasites demonstrating tRNA import was drastically reduced (Fig. 4A). Addition of increasing concentrations of recombinant *Pf*tRip restored tRNA import, presumably by competing for the antibody. At higher *Pf*tRip concentrations, tRNA import ultimately declined because *Pf*tRip also competes for exogenous tRNAs (Fig. 4A).

P. berghei tRip Is Important for Normal Blood-Stage Growth. To assess tRip importance to parasite survival, the tRip-encoding gene (TRIP) was knocked out and replaced in the genome of the WT *P. berghei* ANKA strain by the hDHFR selectable marker and an mCherry cassette via double cross-over homologous recombination (29). Several independent tRip-KO clones were isolated, and successful recombination and the absence of tRip expression were confirmed by Southern and Western blot, respectively (Figs. S6A and S7A).

To confirm that tRNA import in sporozoites is indeed tRip dependent, the tRNA import assay was repeated with tRip-KO sporozoites. As expected, tRNA import was not observed in any tRip-KO sporozoite (>100 sporozoites were examined), consistent with complete ablation of tRNA import had occurred on KO of *TRIP* (Fig. 4B).

To determine whether tRip played any role in blood-stage replication, mice were coinfected with tRip-KO (mCherry$^+$)- and GFP-encoding WT blood-stage parasites. The proportions of red and green fluorescent parasites were scored consecutively for 4 d during the parasite exponential growth phase (Fig. 5A and Fig. S6B). The proportion of tRip-KO parasites decreased at each multiplication cycle compared with WT parasites. Furthermore, the tRip-KO parasite was completely absent in mouse blood after only
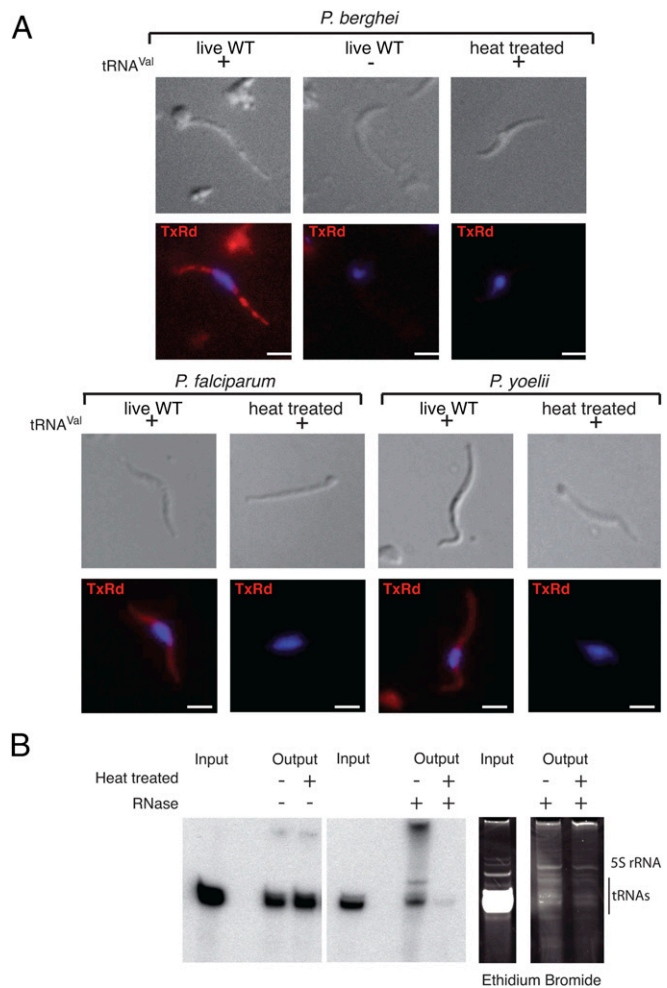

Fig. 3. Import of tRNAs in *Plasmodium* sporozoites. (A) *P. berghei, P. yoelii,* and *P. falciparum* WT sporozoites were incubated with (+) or without (−) *E. coli* tRNA^{Val} and were subjected to FISH. Due to high sequence similarities between mammalian and plasmodial tRNAs, *E. coli* tRNA^{Val} was chosen as a template so that a specific FISH probe could be designed [3′ end-labeled with Texas Red (TxRd)] that does not cross-hybridize with any *Plasmodium* endogenous tRNAs. On tRNA import, about 80% of sporozoites (WT *P. berghei, P. yoelii,* and *P. falciparum*) hybridized the fluorescent probe. (Scale bars, 2 μm.) (B) Radioactive tRNAs from mouse Hepa1-6 cells were cosedimented with both infectious and noninfectious *P. berghei* sporozoites in the absence (*Left*) and presence (*Center* and *Right*) of RNase A. Following extracellular RNase treatment, intracellular sporozoite endogenous tRNAs were undamaged (*Right*), and exogenously added radiolabeled tRNAs were observed within living sporozoites only (*Center*), indicating tRNA import had occurred. Additional bands correspond to tRNA aggregation resulting from phenol extraction.

four successive passages (Fig. 5B). Thus, tRip appears to confer a selective advantage to the parasite during blood-stage infection.

We hypothesized that this phenotype might be a consequence of reduced translational activity in blood-stage tRip-KO parasites. To test this hypothesis, metabolic labeling was performed with [^{35}S] methionine. After 2 and 4 h, equal amounts of [^{35}S]-labeled parasites were analyzed by SDS/PAGE (Fig. S6C). WT and tRip-KO parasites showed the same translational profiles, with more intense labeling for WT, suggesting that translation is globally reduced in the absence of tRip.

To test whether tRip-KO parasites displayed any other phenotype during the parasite life cycle, *Anopheles stephensi* mosquitoes were infected with blood-stage parasites. tRip-KO clones developed normally inside mosquito midguts (Fig. S7B) and yielded normal numbers of sporozoites in mosquito salivary glands
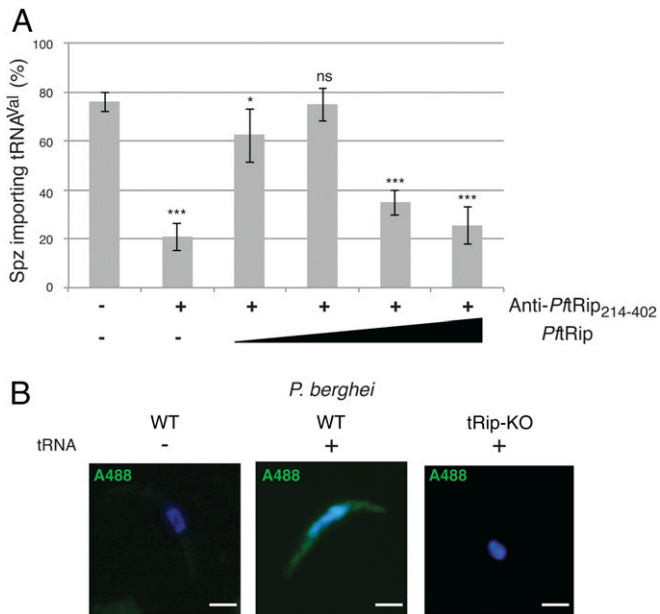
BIOCHEMISTRY

Fig. 4. tRip triggers tRNA import. (*A*) Import of tRNAs in *P. berghei* WT sporozoites was inhibited in the presence of anti-*Pft*Rip$_{214–402}$ antibody. It was gradually rescued following the addition of low concentrations of recombinant *Pft*Rip protein (80 and 160 nM). Higher *Pft*Rip concentrations (320 and 760 nM) lead to tRNA sequestration thereby reducing import. Values correspond to the percentage of tRNA-importing sporozoites (*n* = 50), means are from three independent experiments, error bars are SDs, unpaired *t* test: *$P < 0.05$, **$P < 0.01$, ***$P < 0.001$, ns indicates that values are not significantly different ($P > 0.1$). (*B*) *P. berghei* WT and tRip-KO sporozoites were incubated with (+) or without (−) *E. coli* tRNA^{Val} and were subjected to FISH. Because the tRip-KO parasite expresses mCherry, the probe was 3′ end-labeled with Alexa Fluor 488 (A488). (Scale bars, 2 μm.)

(Fig. S7C). Sporozoite infectivity in vivo was then measured by comparing prepatent periods of infection following i.v. injection of 5×10^3 WT or mutant salivary gland sporozoites (per 4-wk-old C57BL/6 mouse, five mice per group). Blood-stage parasites were detected in all mice 3 d after injection, and parasitemia at day 4 was indistinguishable between WT and tRip-KO (cl4) parasites (~0.06% each), indicating that tRip-KO sporozoites induce a normal pre-erythrocytic phase in the mouse (Fig. S7D). In vitro, tRip-KO parasites developed efficiently inside HepG2 hepatoma cells, releasing similar numbers of merozoites as WT parasites (Fig. S7 *E–G*). Therefore, the lack of tRip in *P. berghei* appears to affect the growth of only blood-stage parasites.

Discussion

Our findings demonstrate a direct connection between tRip and tRNA import in *Plasmodium*. This discovery not only reveals unsuspected molecular exchanges between the parasite and its host, but is also the first report, to our knowledge, of intracellular import of exogenous tRNA in any cell.

We find that *P. falciparum* tRip specifically binds human tRNAs, through its C-terminal domain, with affinity similar to that of well-characterized tRNA-binding proteins such as Trbp111 (7) and ARC1p (11). In agreement with transcriptomic and proteomic data (plasmodb.org/plasmo/), immunolocalization data in *P. berghei* indicate that tRip is expressed throughout the *Plasmodium* life cycle, in intra- and extracellular stages (Fig. S4C), and is integral to the plasma membrane of the sporozoite and blood stages (Fig. 2). Crucially, WT *P. berghei* sporozoites, and presumably other parasite stages as well, can import exogenous tRNAs (Fig. 3), but this capability is lost on disruption of tRip expression (Fig. 4). Together, these data indicate that the

malaria parasite has the ability to import exogenous tRNAs via a tRip-dependent pathway. Host tRNAs would help parasite protein synthesis, provided (*i*) they are substrates for plasmodial aminoacyl-tRNA synthetases or (*ii*) they import bound host aminoacyl-tRNA synthetase (we observed formation of such a ternary complex between AspRS, tRNA^{Asp}, and tRip in vitro; Fig. S3C). Imported tRNAs could balance the surprisingly limited expression of endogenous tRNAs or alter a translational bias.

Gene targeting experiments in *P. berghei* indicate that parasites lacking tRip have a specific defect during the blood phase of the parasite life cycle, i.e., the repeated cycles of parasite multiplication inside erythrocytes is defective. Although lack of tRip is not lethal to blood-stage parasites, coinfection experiments in the mouse blood clearly show that the absence of tRip affects the integrity of blood-stage multiplication (Fig. 5). This phenotype is concomitant with globally reduced protein synthesis in tRip-KO blood-stage parasites, consistent with a scenario wherein host tRNAs are required for robust protein synthesis to proceed (Fig. S6C).
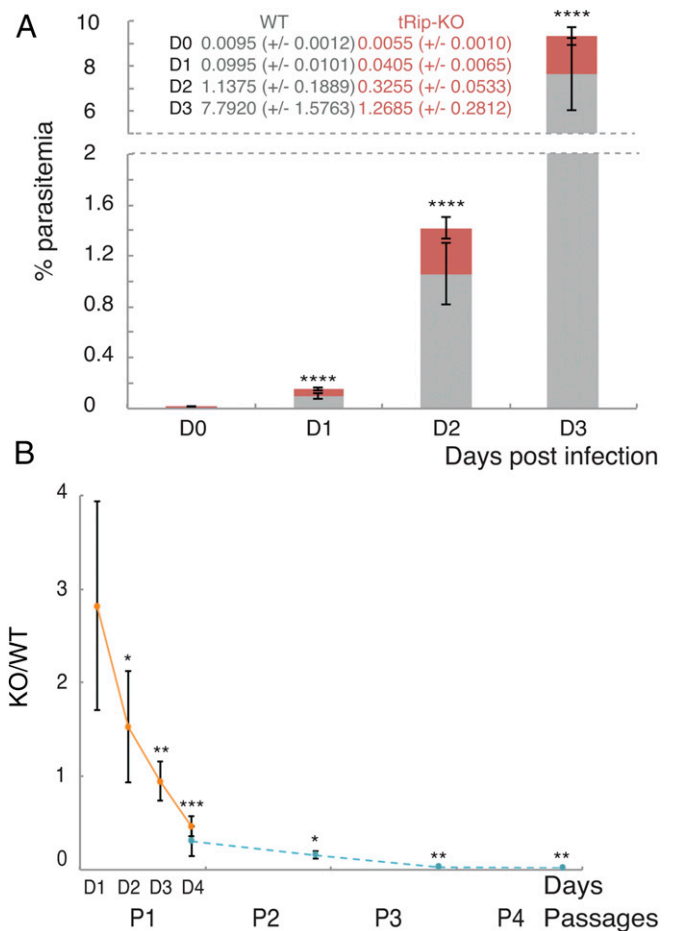

Fig. 5. Phenotype of the tRip-KO parasite. (*A*) Four-week-old mice were coinfected by WT/GFP$^+$ (gray) and tRip-KO/mCherry$^+$ parasites (red). Values correspond to the percentage of red blood cells infected with WT (gray) or tRip-KO (red) parasites, *n* = 15, error bars are SDs, unpaired *t* test: ****$P < 0.0001$. (*B*) Ratio of tRip-KO mCherry$^+$/WT GFP$^+$ parasites in the blood, measured at days 1, 2, 3, and 4 after infection during the course of a first passage (orange) and at day 4 throughout four repeated passages (blue). Values correspond to the ratio of red blood cells infected with tRip-KO parasites to red blood cells infected with WT parasites, at days 1–4 during the first passage (P1, *n* = 6) and at day 4 during the three following passages (P2–P4, *n* = 5), error bars are SDs, unpaired *t* test: *$P < 0.05$, **$P < 0.01$, ***$P < 0.001$.

The observation that tRip is important only during parasite multiplication in the blood is unexpected, from both the parasite stage and host cell perspectives. On the parasite side, why would imported tRNAs be important during the life cycle stage in which multiplication is most limited, and which presumably requires less protein synthesis? Blood-stage parasites only multiply 10-fold per replicative cycle, whereas an oocyst in the mosquito midgut or the liver stage in the mammalian host give rise to tens of thousands of parasite progeny during schizogony (Fig. S4A). In this context, it is interesting to note that orthologs of *Plasmodium* tRip-encoding genes are found only among apicomplexan parasites, which lack an RNA interference pathway (RNAi, except for *T. gondii*) (30). Imported tRNAs may thus serve as a source of regulatory RNAs. In fact, tRNAs and tRNA fragments act as regulatory molecules in other organisms (31–33). Parasites may thus rely on exogenous tRNAs as a growth regulatory mechanism.

On the host cell side, there is no direct evidence for the presence of tRNAs in mature erythrocytes (34). Red blood cells contain no nucleus, and protein biosynthesis is assumed to be absent in these cells. However, mRNAs for the translational machinery are still detected in mature red blood cells (35). Furthermore, many *Plasmodium* species preferentially invade reticulocytes (36), which contain high levels of tRNAs (34) compared with mature erythrocytes (35).

The parasite stage(s) that actually imports the host tRNAs for blood-stage growth remain unknown. Among blood stages, the extracellular merozoite is short-lived and does not traverse host cells, whereas the intraerythrocytic stages resides within a parasitophorous vacuole (PV). Therefore, the most likely hypothesis is that intraerythrocytic parasites pump tRNAs across the PV membrane and, secondarily, across the parasite plasma membrane via tRip. It could also be speculated that tRNAs may be imported during the liver stage or even the sporozoite stage, the only stage that can traverse host cells and thus lie in direct contact with the host cell cytosol and tRNAs, for use in subsequent developmental stages. However, cell traversal-deficient parasites have no defect in invading and developing inside hepatocytes in vivo and in vitro, nor in subsequent development inside erythrocytes (28). We cannot exclude the possibility that tRip, may have a function other than tRNA import during blood-stage growth. For example it might interact with aminoacyl-tRNA synthetases in a manner similar to other Trbp111 homologs such as yeast ARC1p (8), human AIMP1 (9), and *Toxoplasma gondii* Tg-43 (10).

In conclusion, our data describing the tRip-directed import of external tRNAs reveal a novel adaptation of *Plasmodium* parasites to their host, as well as a first occurrence of optimal cell growth dependent on import of exogenous tRNA. Incidentally, tRip function provides a unique molecular system for targeting exogenous molecules into the cytosol of *Plasmodium* cells.

Materials and Methods

Identification of *Pft*Rip Gene. Additional information can be found in *SI Materials and Methods*. The *Pft*Rip gene (PF14_0401) was identified by blasting the yeast ARC1p (NP_011410) and human AIMP1 (NP_004748) sequences against PlasmoDB (plasmodb.org/plasmo/). The sequence alignment was computed with TCoffee software (tcoffee.vital-it.ch/apps/tcoffee/index.html), and the detection of the transmembrane helix was achieved with the PredictProtein software (https://www.predictprotein.org:443/).

***Pft*Rip Cloning and Production.** The *Pft*Rip gene was amplified by PCR from a *P. falciparum* cDNA library (provided by H. Vial, CNRS UMR 5235, University of Montpellier 2, Montpellier, France) and sequenced. Both *Pft*Rip and *Pft*Rip$_{1–174}$ were cloned into pQE30 (Qiagen) to produce proteins with a 6-histidine fusion tags at their N termini. The recombinant *Pft*Rip$_{214–402}$, corresponding to the 260-amino-acid C-terminal domain, was cloned into pGEX-2T (Amersham Biosciences) to yield an N-terminal GST fusion protein. Thrombin cleavage occurred at Proline 214 (instead of the cleavage site provided in pGEX-2T); thus, the C-terminal domain of *Pft*Rip was consequently referred as *Pft*Rip$_{214–402}$. Tagged proteins were purified according to

the manufacturer's instructions on Ni-NTA resin (*Pft*Rip and *Pft*Rip$_{1–174}$, in the presence of 0.005% n-dodecyl β-D-maltopyranoside) or on a gluthatione-Sepharose resin (*Pft*Rip$_{141–402}$) and were further purified by gel filtration (Superdex 200; GE Healthcare) in 50 mM KH$_2$PO$_4$/K$_2$HPO$_4$, pH 7.4, 150 mM KCl, and 10% (vol/vol) glycerol. Gel filtration analysis showed that *Pft*Rip$_{1–174}$ and *Pft*Rip$_{214–402}$ eluted at ∼44 kDa, suggesting that they behaved as homodimers, whereas *Pft*Rip behaved as a tetramer and eluted at ∼158 kDa (based on comparisons to standards).

Enzymatic Footprinting. Yeast native tRNA^{Asp} was 5′ or 3′ labeled as described in refs. 37 and 38, respectively. Assays were performed as described in ref. 38 with 50,000 cpm labeled tRNA, 5 μM *Pft*Rip in 50 mM Hepes, pH 7.4, 10 mM MgCl$_2$, and 25 mM KCl, and 0.01 μg/μL 5S rRNA from *X. laevis*.

Gel Shift Assays. In binding assays, radiolabeled tRNAs (1,000 cpm/μL) were incubated for 20 min on ice in 25 mM Hepes-NaOH, pH 7.4, 5 mM MgCl$_2$, 75 mM KCl, 10% (vol/vol) glycerol, and 20 ng/μL oligo-dT, with increasing concentrations of *Pft*Rip (0–2,000 nM *Pft*Rip; 0–1,000 nM *Pft*Rip$_{214–402}$, and 0–8,000 nM *Pft*Rip$_{1–174}$). In competition assays, labeled tRNA (1,000 cpm/μL) and 30 nM *Pft*Rip$_{214–402}$ were incubated with increasing amounts of unlabeled competitor RNAs (0.625, 1.25, and 2.5 ng/μL total RNA, ribosomal RNAs, or crude tRNAs). Assays were analyzed on an acrylamide/bisacrylamide gel (37.5/1) 6% (wt/vol) in Tris/borate/EDTA buffer, at 140 V for 90 min (*Pft*Rip$_{214–402}$) or 150 min (*Pft*Rip$_{1–402}$) at 4 °C. Radiolabeled yeast tRNA^{Asp} was incubated under the same conditions with either 75 nM yeast AspRS alone and increasing concentrations of *Pft*Rip$_{214–402}$ (12.5, 25, and 50 nM) or 30 nM *Pft*Rip$_{214–402}$ and increasing concentrations of yeast AspRS (37.5, 75, and 150 nM).

Immunofluorescence. Sporozoite membrane extraction was performed as previously described (25). Samples were analyzed with rabbit anti-*Pft*Rip$_{214–402}$ affinity purified using the *Pft*Rip$_{141–402}$ recombinant protein, rabbit anti-GFP antibodies, and mouse anti-CSP serum (39) and detected with anti-rabbit IgG [fluorescein isothiocyanate (FITC)] and anti-mouse IgG [tetramethylrhodamine-isothyocyanate (TRITC)] (Sigma-Aldrich), respectively. Nuclei were spotted with 1 μg/mL DNA stain DAPI (Sigma-Aldrich). Parasites were observed using epifluorescence microscopy (Axiovert200; Zeiss; 100× objective with the corresponding filters).

Air-dried infected erythrocytes were acetone fixed, permeabilized with ice cold methanol, and incubated with rabbit anti-tRip antibodies (1:50 dilution). Mouse anti–MSP-1 antibody was used as a colocalization marker (PEM-2; Santa Cruz Biotechnology). The parasite nuclei were stained with DAPI. Parasites were observed using confocal microscopy (LSM780; Zeiss; 60× objective).

Protease Protection Assays. Infected blood was lysed in PBS containing 0.01% saponin for 5 min on ice. The parasites were washed in PBS and incubated for 30 min at 37 °C in PBS, 1 mM CaCl$_2$, and 6 ng/μL trypsin (Promega), without or with 1% Triton X-100. tRip, AMA-1, and GFP were detected by Western blotting with purified rabbit antibodies raised against the recombinant *Pft*Rip$_{214–402}$, anti–AMA-1 rat antibodies (integral membrane protein control), and anti–GFP-rabbit antibodies (cytosolic control).

Solubility Analysis. Carbonate vs. detergent extraction of membrane proteins was performed on *P. berghei* blood-stage schizonts as described in ref. 40. Parasites were lysed by three cycles of freeze/thaw in 5 mM Tris·HCl, pH 8.0, containing antiprotease mixture (1/100; Sigma-Aldrich) and centrifuged 10 min at 16,000 × g. The membrane-containing pellets were then incubated for 30 min on ice in 0.1 M Na$_2$CO$_3$ (pH 11.5) or 1% Triton and centrifuged for 15 min at 16,000 × g. All fractions were analyzed by Western blot with specific antibodies against *Pft*Rip$_{214–402}$, AMA-1, and GFP.

Import Assays. Sporozoites (2 × 10^4/μL) were first incubated with 0.4 μM radioactive Hepa1-6 tRNAs (50,000 cpm/pmol) in DMEM supplemented with penicillin, streptomycin (Invitrogen), and 1 U/μL RNasin (Promega) for 15 min at room temperature and then washed five times with PBS. After cosedimentation (5 min at 9,000 × g), parasite-bound tRNAs were directly dissolved in loading buffer (20 mM Tris·HCl, pH 7.4, 20 mM EDTA, 8 M urea, and 0.01% of each bromophenol and xylene cyanol dyes) or subjected to RNase A treatment (0.1 μg/μL) for 3 min at 25 °C in PBS and phenol extracted (TRI-Reagent; Sigma-Aldrich) before analysis on a denaturing (8 M urea) PAGE (19/1) 12% (wt/vol). For FISH experiments, to avoid cross-tRNA hybridization, and because its sequence was sufficiently distinct from the parasite's tRNAs, *E. coli* tRNA^{Val} was chosen as a probe. Sporozoites (1 × 10^3/μL) were processed as described previously and subjected to passive sedimentation

Bour et al.

BIOCHEMISTRY

www.manaraa.com

for 1 h at room temperature in cell-line diagnostic microscope slides. The slides were then washed with PBS and air-dried overnight. Samples were fixed with 4% (wt/vol) paraformaldehyde for 15 min, permeabilized with 0.1% Triton X-100 for 10 min at room temperature, and blocked in 2% (wt/vol) BSA, Denhardt's 5×, saline-sodium citrate (SSC) buffer 5×, and 35% (vol/vol) deionized-formamide for 1 h at room temperature. The DNA probes (100 ng/mL; 5′-GAGGTGCTCTCCCAGCTGAGCTAATCACCC-3′) were 3′ end-labeled with Texas Red (TxRd) for probing WT *P. berghei* sporozoites and with Alexa Fluor 488 (A488) for probing tRip-KO sporozoites. Samples were heated at 75 °C for 5 min and incubated together overnight at room temperature in the dark under constant shaking. The slides were washed for 5 min at room temperature with SSC 2× containing 50% (vol/vol) deionized-formamide, and then SSC 2×, SSC 1× containing 1 μg/mL DAPI, and finally SSC 0.5×. Alternatively, sporozoites (1 × 10^3/μL) were preincubated for 15 min at room temperature in the presence of anti-*Pf*tRip$_{214–402}$ (1/50 or 1/20) and increasing concentrations of recombinant *Pf*tRip (80, 160, 320, and 640 nM) before the addition of 0.4 μM *E.coli* tRNA^{Val}.

P. berghei sporozoites (2 × 10^3/μL) were mixed with 0.4 μM Alexa Fluor-labeled in vitro-transcribed *E. coli* tRNA^{Val} or human 5S ribosomal RNA in PBS and RNasin. Immediately after, the mixture (sporozoites and tRNAs) was put between the slide and coverslip with a drop of 0.5% agar/PBS and observed by epifluorescence microscopy.

Parasite Production, Generation of tRip-KO Mutant Parasites, and Phenotyping Procedures. Additional information can be found in *SI Materials and Methods*. All animal experiments were performed in accordance with the CNRS animal care and use committee guidelines.

1. Gardner MJ, et al. (2002) Genome sequence of the human malaria parasite *Plasmodium falciparum*. *Nature* 419(6906):498–511.
2. Filisetti D, et al. (2013) Aminoacylation of *Plasmodium falciparum* tRNA(Asn) and insights in the synthesis of asparagine repeats. *J Biol Chem* 288(51):36361–36371.
3. Hopper AK, Pai DA, Engelke DR (2010) Cellular dynamics of tRNAs and their genes. *FEBS Lett* 584(2):310–317.
4. Salinas T, Duchêne AM, Maréchal-Drouard L (2008) Recent advances in tRNA mitochondrial import. *Trends Biochem Sci* 33(7):320–329.
5. Schneider A (2011) Mitochondrial tRNA import and its consequences for mitochondrial translation. *Annu Rev Biochem* 80:1033–1053.
6. Megel C, et al. (2015) Surveillance and cleavage of eukaryotic tRNAs. *Int J Mol Sci* 16(1):1873–1893.
7. Morales AJ, Swairjo MA, Schimmel P (1999) Structure-specific tRNA-binding protein from the extreme thermophile *Aquifex aeolicus*. *EMBO J* 18(12):3475–3483.
8. Karanasios E, Simos G (2010) Building arks for tRNA: Structure and function of the Arc1p family of non-catalytic tRNA-binding proteins. *FEBS Lett* 584(18):3842–3849.
9. Kim JH, Han JM, Kim S (2014) Protein-protein interactions and multi-component complexes of aminoacyl-tRNA synthetases. *Top Curr Chem* 344:119–144.
10. van Rooyen JM, et al. (2014) Assembly of the novel five-component apicomplexan multi-aminoacyl-tRNA synthetase complex is driven by the hybrid scaffold protein Tg-p43. *PLoS One* 9(2):e89487.
11. Simos G, Sauer A, Fasiolo F, Hurt EC (1998) A conserved domain within Arc1p delivers tRNA to aminoacyl-tRNA synthetases. *Mol Cell* 1(2):235–242.
12. Shalak V, et al. (2001) The EMAPII cytokine is released from the mammalian multi-synthetase complex after cleavage of its p43/proEMAPII component. *J Biol Chem* 276(26):23769–23776.
13. Ruff M, et al. (1991) Class II aminoacyl transfer RNA synthetases: Crystal structure of yeast aspartyl-tRNA synthetase complexed with tRNA(Asp). *Science* 252(5013):1682–1689.
14. Nomanbhoy T, et al. (2001) Simultaneous binding of two proteins to opposite sides of a single transfer RNA. *Nat Struct Biol* 8(4):344–348.
15. Ménard R, et al. (2013) Looking under the skin: The first steps in malarial infection and immunity. *Nat Rev Microbiol* 11(10):701–712.
16. Haldar K, Murphy SC, Milner DA, Taylor TE (2007) Malaria: Mechanisms of erythrocytic infection and pathological correlates of severe disease. *Annu Rev Pathol* 2:217–249.
17. Silvestrini F, et al. (2010) Protein export marks the early phase of gametocytogenesis of the human malaria parasite *Plasmodium falciparum*. *Mol Cell Proteomics* 9(7):1437–1448.
18. Bowyer PW, Simon GM, Cravatt BF, Bogyo M (2011) Global profiling of proteolysis during rupture of *Plasmodium falciparum* from the host erythrocyte. *Mol Cell Proteomics* 10(5):M110001636.
19. Bunnik EM, et al. (2013) Polysome profiling reveals translational control of gene expression in the human malaria parasite *Plasmodium falciparum*. *Genome Biol* 14(11):R128.
20. López-Barragán MJ, et al. (2011) Directional gene expression and antisense transcripts in sexual and asexual stages of *Plasmodium falciparum*. *BMC Genomics* 12:587.
21. Lindner SE, et al. (2013) Total and putative surface proteomics of malaria parasite salivary gland sporozoites. *Mol Cell Proteomics* 12(5):1127–1143.
22. Williams CT, Azad AF (2010) Transcriptional analysis of the pre-erythrocytic stages of the rodent malaria parasite, *Plasmodium yoelii*. *PLoS One* 5(4):e10267.
23. Fritz HM, et al. (2012) Transcriptomic analysis of toxoplasma development reveals many novel functions and structures specific to sporozoites and oocysts. *PLoS One* 7(2):e29998.
24. Mauzy MJ, Enomoto S, Lancto CA, Abrahamsen MS, Rutherford MS (2012) The *Cryptosporidium parvum* transcriptome during in vitro development. *PLoS One* 7(3):e31715.
25. Bergman LW, et al. (2003) Myosin A tail domain interacting protein (MTIP) localizes to the inner membrane complex of *Plasmodium* sporozoites. *J Cell Sci* 116(Pt 1):39–49.
26. Risco-Castillo V, et al. (2015) Malaria sporozoites traverse host cells within transient vacuoles. *Cell Host Microbe* 18(5):593–603.
27. Mota MM, et al. (2001) Migration of *Plasmodium* sporozoites through cells before infection. *Science* 291(5501):141–144.
28. Amino R, et al. (2008) Host cell traversal is important for progression of the malaria parasite through the dermis to the liver. *Cell Host Microbe* 3(2):88–96.
29. Ménard R, Janse C (1997) Gene targeting in malaria parasites. *Methods* 13(2):148–157.
30. Baum J, et al. (2009) Molecular genetics and comparative genomics reveal RNAi is not functional in malaria parasites. *Nucleic Acids Res* 37(11):3788–3798.
31. Mei Y, et al. (2010) tRNA binds to cytochrome c and inhibits caspase activation. *Mol Cell* 37(5):668–678.
32. Ivanov P, Emara MM, Villen J, Gygi SP, Anderson P (2011) Angiogenin-induced tRNA fragments inhibit translation initiation. *Mol Cell* 43(4):613–623.
33. Raina M, Ibba M (2014) tRNAs as regulators of biological processes. *Front Genet* 5:171.
34. Smith DW, McNamara AL (1972) The transfer RNA content of rabbit reticulocytes: Enumeration of the individual species per cell. *Biochim Biophys Acta* 269(1):67–77.
35. Kabanova S, et al. (2009) Gene expression analysis of human red blood cells. *Int J Med Sci* 6(4):156–159.
36. Cromer D, Evans KJ, Schofield L, Davenport MP (2006) Preferential invasion of reticulocytes during late-stage *Plasmodium berghei* infection accounts for reduced circulating reticulocyte levels. *Int J Parasitol* 36(13):1389–1397.
37. Rudinger J, et al. (1992) Determinant nucleotides of yeast tRNA(Asp) interact directly with aspartyl-tRNA synthetase. *Proc Natl Acad Sci USA* 89(13):5882–5886.
38. Frugier M, Moulinier L, Giegé R (2000) A domain in the N-terminal extension of class IIb eukaryotic aminoacyl-tRNA synthetases is important for tRNA binding. *EMBO J* 19(10):2371–2380.
39. Boulanger N, Charoenvit Y, Krettli A, Betschart B (1995) Developmental changes in the circumsporozoite proteins of *Plasmodium berghei* and *P. gallinaceum* in their mosquito vectors. *Parasitol Res* 81(1):58–65.
40. Pachlatko E, et al. (2010) MAHRP2, an exported protein of *Plasmodium falciparum*, is an essential component of Maurer's cleft tethers. *Mol Microbiol* 77(5):1136–1152.
41. Bargieri DY, et al. (2013) Apical membrane antigen 1 mediates apicomplexan parasite attachment but is dispensable for host cell invasion. *Nat Commun* 4:2552.
42. Sinden RE, Butcher GA, Beetsma AL (2002) Maintenance of the *Plasmodium berghei* life cycle. *Methods Mol Med* 72:25–40.
43. Kennedy M, et al. (2012) A rapid and scalable density gradient purification method for *Plasmodium* sporozoites. *Malar J* 11:421–430.
44. Janse CJ, Waters AP (1995) *Plasmodium berghei*: The application of cultivation and purification techniques to molecular studies of malaria parasites. *Parasitol Today* 11(4):138–143.
45. Sinnis P, De La Vega P, Coppi A, Krzych U, Mota MM (2013) Quantification of sporozoite invasion, migration, and development by microscopy and flow cytometry. *Methods Mol Biol* 923:385–400.
46. Sinden RE, Hartley RH, Winger L (1985) The development of *Plasmodium* ookinetes in vitro: An ultrastructural study including a description of meiotic division. *Parasitology* 91(Pt 2):227–244.
47. Deans JA, Thomas AW, Cohen S (1983) Stage-specific protein synthesis by asexual blood stage parasites of *Plasmodium knowlesi*. *Mol Biochem Parasitol* 8(1):31–44.
48. Mellot P, Mechulam Y, Le Corre D, Blanquet S, Fayat G (1989) Identification of an amino acid region supporting specific methionyl-tRNA synthetase: tRNA recognition. *J Mol Biol* 208(3):429–443.
49. Kleeman TA, Wei D, Simpson KL, First EA (1997) Human tyrosyl-tRNA synthetase shares amino acid sequence homology with a putative cytokine. *J Biol Chem* 272(22):14420–14425.
50. Castro de Moura M, et al. (2011) Entamoeba lysyl-tRNA synthetase contains a cytokine-like domain with chemokine activity towards human endothelial cells. *PLoS Negl Trop Dis* 5(11):e1398.
51. Wakasugi K, Schimmel P (1999) Two distinct cytokines released from a human aminoacyl-tRNA synthetase. *Science* 284(5411):147–151.
52. Yang XL, Skene RJ, McRee DE, Schimmel P (2002) Crystal structure of a human aminoacyl-tRNA synthetase cytokine. *Proc Natl Acad Sci USA* 99(24):15369–15374.

Bour et al.

www.manaraa.com